Current Optics and Photonics
Vol. 2, No. 3, June 2018, pp. 221-225

ISSN: 2508-7266(Print) / ISSN: 2508-7274(Online)
DOI: https://doi.org/10.3807/COPP.2018.2.3.221

Protection Method for Diameter-downsized Fiber Bragg Gratings for Highly Sensitive Ultraviolet Light Sensors

Gyeong-Seo Seo and Tae-Jung Ahn*

Department of Photonic Engineering, Chosun University, Gwangju 61452, Korea

(Received February 3, 2018 : revised March 1, 2018 : accepted April 4, 2018)

We suggested the use of miniature hollow glass tubes having high ultraviolet (UV) transmission characteristics for the protection of optical-fiber-type UV sensors. We have recently proposed a highly sensitive optical sensor in the UV spectral range, using a fiber Bragg grating (FBG) coated with an azobenzene polymer as the photoresponsive material. In this study, we used UV-transparent miniature glass tubes to protect the etched FBG with the azobenzene polymer coating. This technique will be very useful for protecting various fiber-based UV sensors.

Keywords : UV sensor, Azobenzene, Fiber Bragg grating, Fiber optic sensor
OCIS codes : (040.7190) Ultraviolet; (060.3738) Fiber Bragg gratings, photosensitivity; (060.2370) Fiber optics sensors; (160.5335) Photosensitive materials

I. INTRODUCTION

Ultraviolet rays are recognized as light that must not come into contact with human body. However, UV light is used in everyday life, and utilization rates have recently been increasing in various industrial fields, such as UV curing, UV purification, and optical semiconductor element fabrication by exposure to UV light [1-3]. Because UV light is invisible, the danger of accidents accompanying its use is high [4]. To reduce such accidents, a UV sensor is necessary. In addition, UV light is emitted by electric leakage and similar situations in lightning strikes and high-power generation, and it is possible to prevent accidents by detecting the UV light before a fire develops [5]. If UV sensors were developed based on semiconductor devices, these would likely cause malfunctions in applications using high voltages. In addition, in the case of optoelectronic devices exhibiting electromagnetic interference (EMI), although power must be supplied to the sensor, there is a limit to how closely the generated UV light can be measured [6, 7]. For these reasons, UV sensors based on optical fibers have been proposed as passive optical sensing elements that would not be affected by EMI, and would not require an internal power supply [8-10]. Traditionally the fiber Bragg grating (FBG) has exhibited unparalleled performance in various optical sensor applications, due to advantages like compact size, high sensitivity, multipoint measurement, and remote measurement [11, 12].

We have recently proposed a UV sensor based on an FBG coated with an azobenzene polymer that mechanically reacts to UV light. This special functional polymer exhibits good absorption in the UV region, as reported by earlier studies [13-16]. When azobenzene absorbs UV light, its internal structure changes reversibly (trans to cis), thereby changing the volume of the material [13, 14]. These volume changes due to UV absorption induce tension in the FBG, linearly increasing the grating period with the increase in the resonant wavelength of the grating. The working principle of the UV sensor involves indirect detection of UV light by measuring and analyzing the change in the grating's central wavelength according to the intensity of the incident UV light [13]. The measurement sensitivity has been dramatically improved by using techniques like etching the FBG to reduce the diameter, so that the tension induced by the UV-exposed azobenzene polymer material changes the grating period more effectively [17]; converging the UV light to

*Corresponding author: taejung.ahn@chosun.ac.kr, ORCID 0000-0001-8801-9846
Color versions of one or more of the figures in this paper are available online.

the FBG sensing region using a cylindrical optical lens in the UV spectral range [18]; and reflecting the afterglow, which has not been absorbed by the polymer coating in the incident light, by means of a curved reflector and reabsorbing it under the optical sensor [19].

However, it is necessary to protect the polymer-coated FBG in air from external dust, temperature deformation, and physical-property changes due to environmental effects, etc., so an appropriate protection method should be devised for fiber-optic UV sensors. In this study, we used UV-transparent miniature hollow glass tubes to physically protect the FBG as a UV sensing element, because the optical element easily bends and deforms. We confirmed the UV measurement characteristics of the sensor for three types of glass tubes with different UV transmission characteristics, and confirmed the possibility of miniaturizing the optical element. In addition, the loss of transmitted light due to the coupling between the cylindrical optical lens and the glass tube was experimentally confirmed and theoretically analyzed.

II. METHODS AND RESULTS

The FBG (SJ Photonics Inc.) used in this study had a grating period of 530 nm and central wavelength of 1548.4 nm. The azobenzene polymer as a photoactive coating material was coated on the etched FBG with a downsized diameter of approximately 80 μm. Details about the preparation of the azobenzene polymer can be found in Ref. [13]. Then we used three kinds of UV-transparent glass tubes (VitroCom Inc.) with different UV transmission spectra: (i) borosilicate, (ii) clear fused quartz, and (iii) synthetic fused silica, respectively called B-glass, Q-glass, and S-glass. The outer and inner diameters of all the tubes were 2.4 and 2.0 mm respectively. Transmittance in the short-wavelength region of 250 nm or below decreases in order from S-glass to Q-glass to B-glass, as shown in Fig. 1. Therefore, we expect that S-glass, with good transmittance at short wavelengths, will provide the highest photoreactivity, compared to the others.

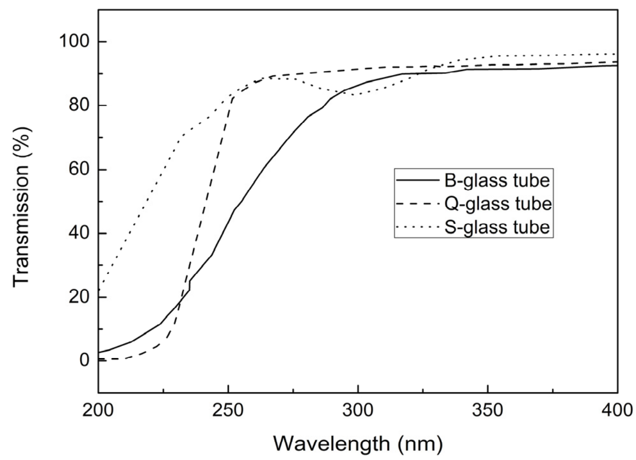

FIG. 1. Transmission spectra of borosilicate, clear fused quartz, and synthetic fused silica glass tubes (refer to specifications of the miniature hollow glass tubing provided by VitroCom Inc.).

A portion of the polymer-coated region of the UV sensor was inserted into each tube, and the same amount of UV radiation was incident on the tubed sensing region. The central-wavelength shift of the FBG sensor was determined by a laboratory-made interrogation system, in which a superluminescent laser diode (SLD) with a central wavelength of 1550 nm and spectral width of 50 nm was used as the light source. Figure 2 illustrates the experimental setup for measuring the FBG's central wavelength with respect to UV exposure. The central wavelength of a reflected light signal is generally shifted to longer wavelengths, due to change in the ambient temperature or tension of the FBG [18]. Reversible tension is induced when UV light is absorbed by the functional polymer coated on the FBG, which shifts the central wavelength associated with the change in the grating period. Figure 3 shows an example of the shift in the FBG's resonance spectrum with UV exposure. The four curves show the continuous movement of the central wavelength of the FBG toward longer wavelengths under UV exposure of 4 mW/cm^2 intensity for 28 s.

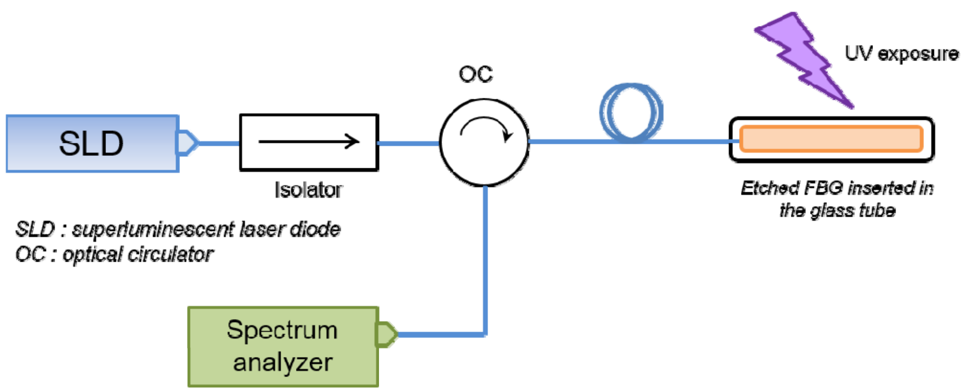

FIG. 2. Measurement configuration with the interrogation system for FBG sensors: etched FBG coated with the azobenzene polymer (left), and the sensor inserted into the UV glass tube (right).

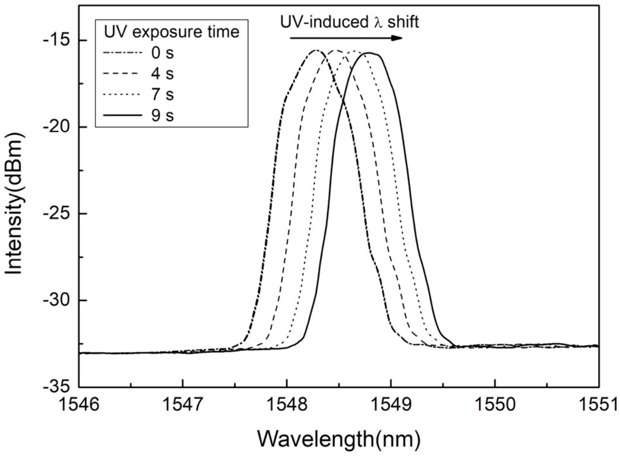

FIG. 3. Central-wavelength shift of the FBG sensor during UV exposure.

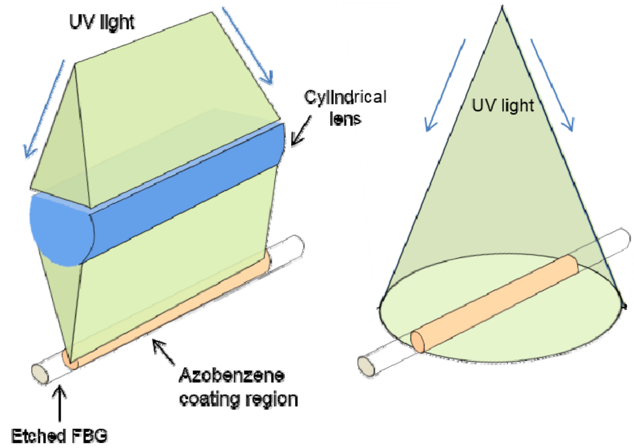

(a) (b)

FIG. 4. Schematic of UV light measurements, with and without a cylindrical focusing lens.

This experiment was carried out with consideration of the UV-transparent cylindrical focusing lens effect. We used a UV condensing lens (LJ4107-UV, Thorlabs Inc.). To improve the highest sensitivity, we decided to locate the FBG sensor at a position 1 mm above the focal length of the lens, because the focused UV light fully covers the active sensing-coating region at that position (Fig. 4(a)). In addition, experiments without the lenses were carried out, with the exposure area of UV light sufficiently containing the azobenzene polymer region of the FBG (Fig. 4(b)).

Using an equipment-control program, a UV lamp (A4000 UltraCure, EFOS Acticure Inc.) with a power of 100 W and wavelength of 250~450 nm was repeatedly turned on and off, and the optical sensor under test was exposed to UV light every 60 s. This operation was repeated three times in succession, to measure the degree of UV reaction of the photosensor. For high-accuracy measurement, power operation of the UV lamp and data acquisition were implemented programmatically. When the UV was turned on, the wavelength-shifting behavior shown in Fig. 3 was measured in real time, as shown in Fig. 5.

The three types of UV-transmitting glass tubes exhibited similar reactions and showed the same result, regardless of the cylindrical lenses. This is because the tube thickness of 0.2 mm is low, and the UV absorption effect can be ignored. Therefore, it is effective to use B-glass for the protective tube for the photosensor, because the cost efficiency of the B-glass tube is about twice that of Q-glass and five times that of S-glass, while exhibiting similar characteristics.

When comparing the cases of the absence of a tube using the lens to the presence of a tube, the maximum rate of wavelength change decreases by about 5%, as shown in Fig. 5(a), while in contrast it decreases by 16% without using the lens, as shown in Fig. 5(b). The decrease depends on the change in UV transmission through the glass tube,

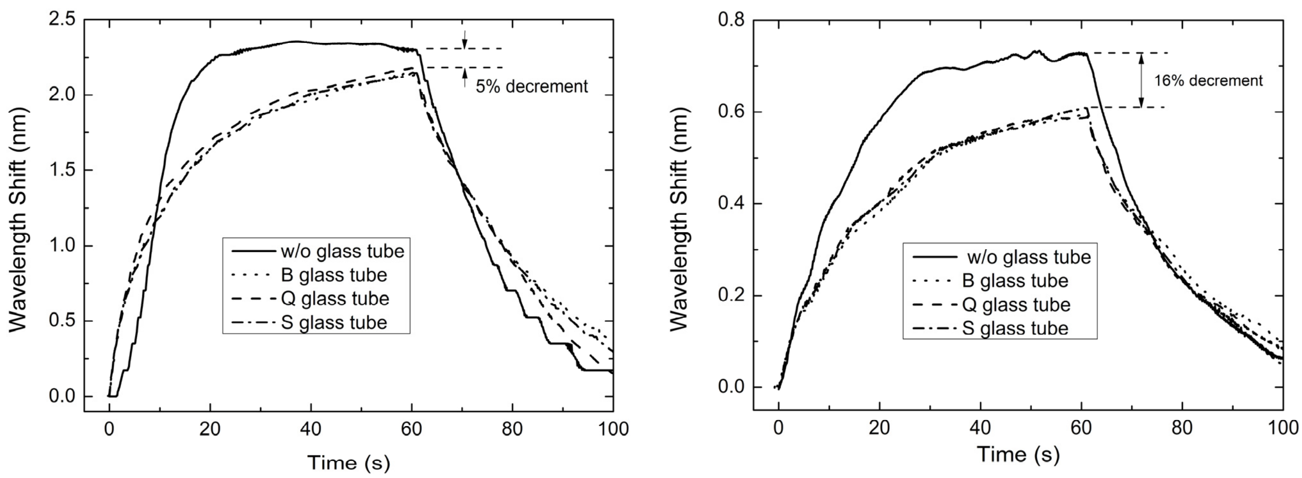

(a) (b)

FIG. 5. UV responsivity of the FBG sensor inserted into the various glass tubes, (a) with and (b) without a focusing lens, compared to the FBG sensor with no tube.

due to absorption and/or reflection in the tube. Assuming that the UV absorption of the very-low-thickness glass tubes is small, the drop in UV response depends only on the reflection effect on the glass tube, with or without the focusing lens.

Figure 6 shows schematics of a glass tube, according to whether or not the lens is used in the theoretical analysis. When no condenser lens is used, h is the height between the starting point of the UV light and the center of the tube, r is the radius of the tube, d is the tube's thickness, and θ is the angle of incidence for any x and y-axis. If the lens shown in Fig. 6(a) is used, because it is at normal incidence θ = 0, and the reflectance R is given by

$$R=\left(\frac{n_2-n_1}{n_2+n_1}\right)^2, \tag{1}$$

where n_1 and n_2 are the refractive indices of air and the glass respectively. The refractive index of the tube's glass is set to 1.4585, equivalent to that of fused silica [20]. Using Eq. (1) and $R_{tot}=R\{1+(1-R)/(1+R)\}$ for the sum of the geometric sequence for multiple reflection (assuming that the reflectances of the outer and inner surfaces were equal and the thickness was large enough than the coherence length of the input UV light source to ignore a phase relations in the formula), the total reflectance R_{tot} of the glass tube is estimated as 6.72%, for comparison to the experimental result of 5% in Fig. 5(a).

In the case where the lens is not used, as shown in Fig. 6(b), from the calculation using the trigonometric triangular ratio and the Fresnel equation [21]:

$$\tan A=\frac{x}{h-y},\ \tan B=\frac{x}{y} \tag{2}$$

$$\theta=A+B=\tan^{-1}\left(\frac{x}{h-y}\right)+\tan^{-1}\left(\frac{x}{y}\right) \tag{3}$$

$$\theta'=\sin^{-1}\left(\frac{n_1}{n_2}\sin\theta\right) \tag{4}$$

$$\beta=\theta'+\tan^{-1}\left(\frac{d}{r}\tan\theta'\right) \tag{5}$$

The reflectance was theoretically estimated to be about 28%, using incident angles at the outer and inner surfaces of the glass tube (Eq. (2)) and Fresnel equations [21] considering multiple reflection from the inner and outer surfaces. It was confirmed that the experimental value of 16% in Fig. 5(b) differs by about 12% from the calculated value. This is because the calculation is based on the assumption of equal amounts of transverse electric and transverse magnetic polarized light, unlike the polarized light actually emitted from the UV source. It has been reported that the focused UV light from a cylindrical lens increases the photosensitivity of the optical sensor [18]. In this study, we also observed that the focused light is efficient even when using the glass tube to protect the FBG sensor as a passive UV-sensing element, because of the UV transmission characteristics related to the Fresnel reflections.

III. CONCLUSION

In this study, we conducted an experiment to select a type of UV-transparent glass tube for the physical protection of a highly sensitive UV sensor based on a diameter-downsized FBG coated with an azobenzene polymer. To determine the best glass for the UV sensor, we tested the UV-induced responses of the FBG inserted in each of three glass tubes. All of the tubes tested exhibited similar characteristics, but B-glass is about 3-5 times more economical than the other glass types. In addition, it was observed that it is effective to use a UV-focusing lens, based on the result that the response when using the glass tube also exhibits a decreasing trend: When the lens is used, 5% is the maximum difference of the UV-induced wavelength shift in the presence or the absence of the glass tube, whereas it is 16% when the lens it not used. We found that it is useful to combine the B-glass tube with the cylindrical focusing lens in the UV region, to physically protect the fiber-optic UV sensor while maintaining its detection sensitivity.

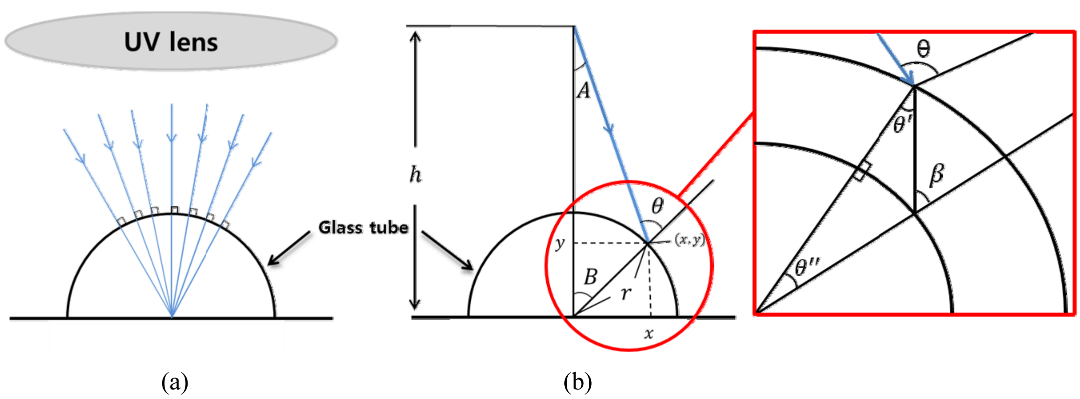

FIG. 6. Schematic for the analysis of reflection effects of UV light in a glass tube, (a) with and (b) without the focusing lens.

ACKNOWLEDGMENT

Funding: This work was supported by the Future Creative Science Division of 2017; the Korean Research Foundation's mid-career researcher support project [grant number 2017R1 A2B2006565]; and the Korea Energy Technology Evaluation Institute (KETEP) Energy Human Resources Development [grant number 20174030201620].

REFERENCES

1. S. P. Pappas, *UV Curing: Science and Technology, Vol. 2*, Technology Marketing Corp. (1985).
2. B. Srikanth, "Recent advancements in UV technology yield enhanced TOC reduction performance," Ultrapure Water **15**, 40-46 (1998).
3. B. J. Lin, "Deep UV lithography," J. Vacuum Sci. Technol. **12**, 1317-1320 (1975).
4. A. F. Nichols, T. Itoh, J. A. Graham, W. Liu, M. Yamaizumi, and S. Linn, "Human damage-specific DNA-binding protein p48: Characterization of XPE mutations and regulation following UV irradiation," J. Biol. Chem. **275**, 21422-21428 (2000).
5. Y. Hu and K. Liu, *Inspection and Monitoring Technologies of Transmission Lines with Remote Sensing* (Academic Press, 2017), Chapter 4.
6. J. Kim, "The strength of surface UV radiation over Korea peninsula and the consequent Minimum Erythema Dose (MED) and its exposure time for Korean skin type and reaction," Institute of Earth & Environment Yonsei University, Health Care Technology Research and Development Project Report (2001), p. 3.
7. C. Cao, C. Hu, X. Wang, S. Wang, Y. Tian, and H. Zhang, "UV sensor based on TiO_2 nanorod arrays on FTO thin film," Sens. Actuators, B **156**, 114-119 (2011).
8. A. V. Joža, J. S. Bajić, D. Z. Stupar, M. P. Slankamenac, M. Jelić, and M. B. Živanov, "Simple and low-cost fiber-optic sensor for detection of UV radiation," Telfor J. **4**, 133-137 (2012).
9. Y. Kim, S. Ju, S. Jeong, and W.-T. Han, "Photonic properties of Ti-doped optical fiber," J. Nonlinear Opt. Phys. Mater. **19**, 781-790 (2010).
10. K. T. Kim, N. I. Moon, and H.-K. Kim, "A fiber-optic UV sensor based on a side-polished single mode fiber covered with Azobenzene dye-doped polycarbonate," Sens. Actuators, A **160**, 19-21 (2010).
11. A. Othonos and K. Kalli, *Fiber Bragg Gratings: Fundamentals and Applications in Telecommunications and Sensing* (Artech House Optoelectronics Library, 1999), Chapter 7.
12. S. R. Oh, D. Kang, J. Choi, J. H. Kim, H. Lee, K-S. Kim, and S. Kim, "Supercontinuum notch shaping via fiber Bragg grating for the excitation source in coherent anti-stokes Raman spectroscopy," in *Proc. Conference on Lasers and Electro-Optics/Pacific Rim 2015* (Korea, Aug. 2015), paper 26C3_7.
13. H.-K. Kim, W. Shin, and T.-J. Ahn, "UV sensor based on photomechanically functional polymer-coated FBG," IEEE Photon. Technol. Lett. **22**, 1404-1406 (2010).
14. D.-S. Choi, H.-K. Kim, and T.-J. Ahn, "The study of thermal effect suppression and wavelength dependence of azobenzene-coated FBG for UV sensing application," Korean J. Opt. Photon. **22**, 67-71 (2011).
15. H.-K. Kim, X.-S. Wang, Y. Fujita, A. Sudo, H. Nishida, M. Fujii, and T. Endo, "Reversible photo-mechanical switching behavior of azobenzene-containing semi-interpenetrating network under UV and visible light irradiation," Macromol. Chem. Phys. **206**, 2106-2111 (2005).
16. S. K. Rastogi, H. E. Anderson, J. Lamas, S. Barret, T. Cantu, S. Zauscher, W. J. Brittain, and T. Betancourt, "Enhanced release of molecules upon ultraviolet (UV) light irradiation from photoresponsive hydrogels prepared from bifunctional azobenzene and four-arm poly (ethylene glycol)," ACS Appl. Mater. Interfaces Article ASAP DOI: 10.1021/acsami.6b16183 (2017).
17. I.-S. Song, C.-Y. Kim, H-K. Kim, B.-H. Kim, and T.-J. Ahn, "Sensitivity improvement of UV FBG sensor by downsizing grating diameter," in Proc. SPIE **8924**, 892406 (2013).
18. I.-S. Song, W.-Y. Kim, C.-Y. Kim, B. H. Kim, H.-K. Kim, and T.-J. Ahn, "Sensitivity enhancement of a UV photo-sensor based on a fiber Bragg grating coated by a photo-mechanical functional polymer," Sens. Actuators, A **232**, 223-228 (2015).
19. W. Y. Kim, C.-Y. Kim, H.-K. Kim, and T.-J. Ahn, "Improving the sensitivity of an ultraviolet optical sensor based on a fiber Bragg grating by coating with a photoresponsive material," Korean J. Opt. Photon. **26**, 83-87 (2015).
20. I. H. Malitson, "Interspecimen comparison of the refractive index of fused silica," J. Opt. Soc. Am. **55**, 1205-1209 (1965).
21. S. O. Kasap, *Optoelectronics and Photonics* (2nd Edition, Pearson, 2013), Chapter 1, p. 42.